AIP Journal of Applied Physics

Adaptive ferroelectric states in systems with low domain wall energy: Tetragonal microdomains

Y. M. Jin, Y. U. Wang, A. G. Khachaturyan, J. F. Li, and D. Viehland

Citation: Journal of Applied Physics **94**, 3629 (2003); doi: 10.1063/1.1599632
View online: http://dx.doi.org/10.1063/1.1599632
View Table of Contents: http://scitation.aip.org/content/aip/journal/jap/94/5?ver=pdfcov
Published by the AIP Publishing

Adaptive ferroelectric states in systems with low domain wall energy: Tetragonal microdomains

Y. M. Jin, Y. U. Wang, and A. G. Khachaturyan[a)]
Department of Ceramic and Materials Engineering, Rutgers University, 607 Taylor Road, Piscataway, New Jersey 08854

J. F. Li and D. Viehland
Department of Materials Science and Engineering, Virginia Tech, Blacksburg, Virginia 24061

(Received 27 February 2003; accepted 18 June 2003)

Ferroelectric and ferroelastic phases with very low domain wall energies have been shown to form miniaturized microdomain structures. A theory of an adaptive ferroelectric phase has been developed to predict the microdomain-averaged crystal lattice parameters of this structurally inhomogeneous state. The theory is an extension of conventional martensite theory, applied to ferroelectric systems with very low domain wall energies. The case of ferroelectric microdomains of tetragonal symmetry is considered. It is shown for such a case that a nanoscale coherent mixture of microdomains can be interpreted as an adaptive ferroelectric phase, whose microdomain-averaged crystal lattice is monoclinic. The crystal lattice parameters of this monoclinic phase are self-adjusting parameters, which minimize the transformation stress. Self-adjustment is achieved by application of the invariant plane strain to the parent cubic lattice, and the value of the self-adjusted parameters is a linear superposition of the lattice constants of the parent and product phases. Experimental investigations of $Pb(Mg_{1/3}Nb_{2/3})O_3-PbTiO_3$ and $Pb(Zn_{1/3}Nb_{2/3})O_3-PbTiO_3$ single crystals confirm many of the predictions of this theory. © *2003 American Institute of Physics*. [DOI: 10.1063/1.1599632]

I. INTRODUCTION

The ferroelastic and/or martensite microstructure consists of polydomain plates. Each plate is formed by alternating layers of twin-related domains, where the layers are parallel to the twin plane. The structure of a polydomain martensite plate is schematically shown in Fig. 1(a). Because the boundary between twin-related domain layers [shown by white and black stripes in Fig. 1(a)] is the twin plane, there is no crystal lattice misfit between layers. The relative thicknesses of the domain layers can be adjusted to establish the macroscopic invariance of the habit plane,[1,2] and in so doing eliminates long-range stress fields generated by crystal lattice misfits.[3–5] This requires the domain-averaged stress-free transformation strain of each plate to be an invariant plane strain (IPS), where the invariant plane is parallel to the habit plane.

Stress-accommodating domain structures typical of martensite should also occur for any displacive transformation, which can form a domain-averaged transformation strain that is an IPS. An example of such a polydomain structure for the tetragonal phase of an ordered CuAu alloy is shown in Fig. 1(b).[6] The black and white stripes in this transmission electron microscopy (TEM) image are alternating twin-related domains of the tetragonal phase. These stripes assemble into macroplates of the kind shown in Fig. 1(a), which are in turn arranged into a larger scale pattern.

a)Electronic mail: khach@jove.rutgers.edu

A. Ferroelastics with very low domain wall energy: Adaptive martensite

The crystal lattice parameters of individual martensite domains are those of the low temperature transformed state. However, a unique situation can arise in the case of a very low domain boundary energy: *domains can miniaturize, as the domain size is proportional to* $\sqrt{\gamma}$*, where* γ *is the domain wall energy*. A thermodynamic and crystallographic theory[7,8] has been developed for this unique case, and applied to explain unusual features of an intermediate martensitic phase previously observed in both Al–62.5%Ni (Ref. 9) and Fe–Pd (Ref. 10) alloys. In this case of miniaturized domains, the crystal lattice parameters measured in the conventional diffraction experiment are no longer the parameters of the low temperature transformed state forming the miniaturized domains (microdomains). Rather, the lattice parameters are a combination of those of different orientation variants of the microdomains, as determined by the IPS. As a consequence, the lattice parameters themselves follow the twinning rules. We use the term ''adaptive phase'' to describe this unique structurally mixed state.

The adaptive phase is a particular (miniaturized) case of conventional martensite with stress-accommodating domains, which can only be expected in situations where the domain wall energy is abnormally small. In this case, the IPS is fully determined by a combination of the lattice parameters of the low symmetry phase (which forms microdomains) and the high symmetry parent phase. There is no other kind of phase that could have this unique property. Therefore, if the stress-free transformation strain calculated

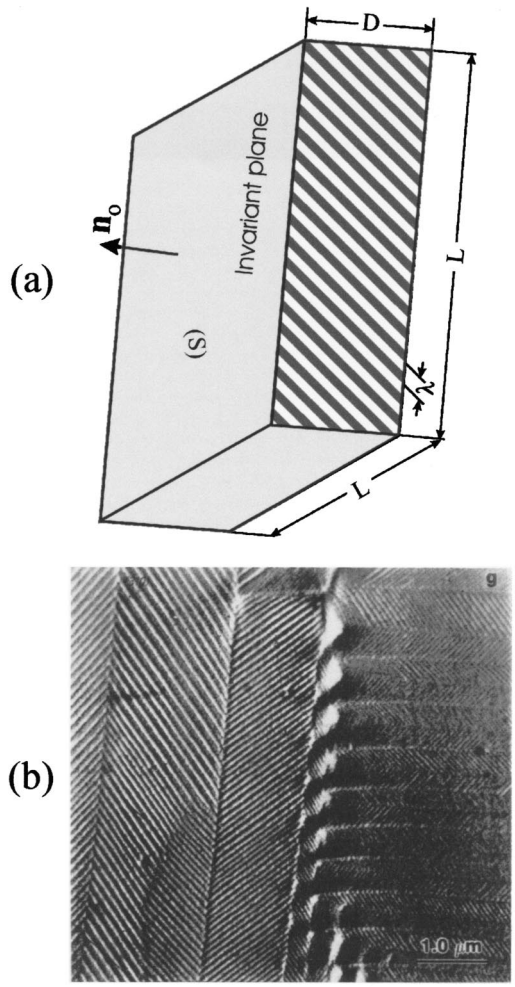

FIG. 1. (a) Structure of a polydomain martensitic plate consisting of alternating lamellas of two twin-related orientation variants (domains) of the martensite shown by black and white. The boundary between the lamellas is the twin plane. The ratio of the ''black'' and ''white'' domain thicknesses provides the macroscopic invariancy of the habit plane. (b) Dark-field TEM image of the strain-accommodating domain structure in CuAu alloy (see Ref. 6). Alternating white and black stripes are images of the (110) twin-related tetragonal domains (orientation variants) of the $L1_0$ ordered phase with the alternating directions of the tetragonal axis *c*. They are arranged in the plates similar to that shown in (a). These plates fully fill a sample.

from the crystal lattice parameters of the low temperature and parent phases is the IPS, it can safely be concluded that the martensite phase is the adaptive type. The volume fractions of the various microdomains (i.e., nanosized orientation variants of conventional martensite) can change in response to applied stress σ and external boundary conditions. Thus, in the adaptive phase, the crystal lattice parameters (which are microdomain averaged over the plate) are continuously adjusted by σ.

Unlike a conventional martensite phase, the crystal lattice of the adaptive phase can be considered homogeneous only above a scale of ~10 nm. At and below this length, the structure is inhomogeneous: it is a mixed state, consisting of alternating stress-accommodating coherent structural microdomains (i.e., nanosized orientation variants of conventional martensite). The spatial distribution (i.e., patterning) of microdomains comprising the adaptive phase is determined by the same condition as that of conventional martensite[3–5]—minimization of the sum of the transformation-induced strain and interfacial domain wall energies. If the adaptive phase is formed from tetragonal microdomains, then the domain structure schematically shown in Fig. 1(a) will be conformally miniaturized. Accordingly, the black and white stripes in Fig. 1(b) [which are the differently oriented (110) twin-related tetragonal domains] would become the *microdomains* of the adaptive phase, and the plates composed of these microdomains, schematically shown in Fig. 1(a), would become *macrodomains* of the adaptive phase.

Since the adaptive phase is the particular case of a martensitic domain structure with a very low γ, the physical properties of the adaptive phase will be similar to those of conventional martensite having stress-accommodating domains. The fingerprints of the adaptive martensite phase include: (i) an interdependence of the crystal lattice parameters on those of the parent cubic phase and those forming the microdomains; (ii) shape memory effects; and (iii) a dependence on thermal and stress history (i.e., nonergodicity).

B. Ferroelectrics with low domain wall energy: Adaptive ferroelectrics

Ferroelectric transformations are another important class of materials with displacive crystal lattice rearrangements, where adaptive phases might form. Ferroelectric domains are crystallographically equivalent orientation variants. They are structural domains with polarization **P**. To accommodate crystal lattice misfits, structural domains self-assemble into a martensite-like pattern. The presence of polarization in structural domains will not change the pattern, if neighboring domains are separated by a twin plane boundary (which is the case), and if the twin-related polarization vectors of neighboring domains are directed in a ''head-to-tail'' fashion. In this case, the gradient of the polarization at the domain boundaries does not generate an electrostatic field (i.e., uncharged domain walls). Accordingly, ferroelectric domains are simultaneously structural ones, provided that the self-assembly pattern eliminates both the strain and electrostatic energies.

Similar to martensitic transformations, a significant reduction in γ will result in domain miniaturization. In such a ferroelectric adaptive phase, both the observed macrodomain polarization and crystal lattice parameters will be microdomain-averaged. The total dipole moment of the adaptive phase is a vector sum of the moments of alternating polar microdomains that compose the macrodomains. It is a weighted sum of the relative thicknesses, ω and $1-\omega$, of the microdomain variant populations. Accordingly, the polarization direction in the adaptive phase will depend on the ratio of the thicknesses of twin-related microdomains. Thus, the polarization direction will not coincide with any fixed high symmetry direction. The observed polarization and crystal lattice parameters will be of the same symmetry, but one with a point group that is reduced to only those symmetry elements common to both the parent cubic and low temperature product phases.

A ferroelectric adaptive phase (consisting of miniaturized domains that are simultaneously polar and structural)

should have properties similar to those of a martensitic adaptive phase (with no polarization), plus several additional properties inherent to the presence of polarization in the microdomains. The effect of electric field **E** and mechanical stress σ on an adaptive ferroelectric should be similar, both resulting in a redistribution of the microdomain variant populations. Under **E**, the volume fraction of microdomains with a favorably oriented polarization will increase, and that of microdomains which are unfavorably oriented will decrease. This will produce a macroscopic shape change, which will be on the order of the transformation strain. The electric field-induced microdomain rearrangement will affect the crystal lattice parameters of the adaptive phase, resulting in an abnormally high piezoelectricity, which is much greater than that of a homogeneous domain state. Because the microdomain-averaged polarization will depend on the ratio of microdomain thicknesses, an **E**-induced change in this ratio should result in a change in the polarization direction. The direction of the microdomain-averaged polarization will rotate under electric field. No such continuous rotation of the polarization vector is known in a conventional homogeneous ferroelectric domain.

The fingerprints of a ferroelectric adaptive phase are: (i) the IPS that is fully determined by a combination of the lattice parameters of the low symmetry product phase (forming microdomains) and the high symmetry parent phase; (ii) the variant populations are variable with **E** and σ, resulting in abnormally high piezoelectricity; (iii) a gradual rotation of the polarization vector and change in its magnitude upon gradual change of the electric field and/or applied stress; and (iv) shape memory effects, and shape memory polarization. Furthermore, since the domain walls are very mobile due to the very low domain wall energy, the $P-E$ and $\epsilon-E$ hysteresis loops for these materials are expected to be very slim.

These fingerprint properties of adaptive ferroelectrics are, in particular, interesting in regard to recent reports of new monoclinic ferroelectric phases (FE_m) in oriented poled $Pb(Mg_{1/3}Nb_{2/3})O_3-PbTiO_3$ (PMN–PT) and $Pb(Zn_{1/3}Nb_{2/3})O_3-PbTiO_3$ (PZN–PT) crystals.[11–14] New FE_m phases have been reported near a morphotropic boundary (MPB), which separates the phase fields of tetragonal (FE_t) and rhombohedral (FE_r) ferroelectric phases in the phase diagrams. One phase has the polarization vector confined to the $(010)_c$ plane, while the other has it confined to $(011)_c$. A common feature of these FE_m phases is extremely high electromechanical constants, as the electrostrictive deformation is close to the transformation strain.[15–17] These high electromechanical coefficients have been explained on the basis of a polarization rotation mechanism.[11] It should be emphasized that these pronounced features of the adaptivity are expected due to the easy rearrangement of microdomains under applied **E**.

In this article, it will be shown that the special properties of the FE_m phases in PMN–PT and PZN–PT can be explained as a consequence of adaptive phases formed by stress- and depolarization electric field-accommodating microdomains of the FE_t phase. In addition, the crystal lattice parameters of the FE_m (pseudo-orthorhombic) phase have been found to be close to those predicted by the theory of the adaptive phase.[18] Also, the required assumption of a low domain wall energy for adaptive phase formation is in agreement with the fact that the stability field of these FE_m phases is sandwiched in the vicinity of the MPB between the FE_t and FE_r phases. Together, these observations make a strong case in favor of the assumption that the FE_m phases observed near the MPB in PMN–PT and PZN–PT are adaptive phases, with a mixed nanoscale structure.

II. STRUCTURAL PROPERTIES OF AN ADAPTIVE PHASE CONSISTING OF TETRAGONAL MICRODOMAINS

As mentioned above, the adaptive phase is a particular case of stress-accommodating domain structure that is conformally miniaturized to the nanoscale level. The theory is based upon abnormally small domain wall energies. Minimization of the sum of the strain and interfacial energies produces structural domains assembled in a polydomain plate, as illustrated in Fig. 1(a). The typical domain size λ_0 is related to the thickness of the polydomain plate D and the domain wall energy γ by the relationship

$$\lambda_0 = \beta \sqrt{\frac{\gamma}{\mu \epsilon_0^2} D}, \tag{1}$$

where β is a dimensionless constant, μ is the shear modulus, and ϵ_0 is the twinning strain transforming one domain into its twin-related counterpart.[3,4] It is important that the typical thicknesses of ferroelectric and ferromagnetic domains in a plate of thickness D [see Fig. 1(a)] are also described by a similar relationship that is proportional to $\sqrt{\gamma D}$. This is a profound analogy between structural and ferroelectric domains, which is important to adaptive ferroelectric phase formation.

It follows from Eq. (1) that if $\gamma \to 0$, then $\lambda_0 \to 0$ as well. This demonstrates that a reduction of the domain wall energy results in domain miniaturization. If γ is sufficiently small, miniaturization can reach a limit where the domain layer thickness λ_0 [shown in Fig. 1(a) by white and black stripes] approaches the nano- and/or atomic scale.

As is well known, diffraction from structural domains with twin-related orientations results in a splitting of diffraction spots, along the direction that is perpendicular to the twinning plane. To be able to determine the crystal lattice parameters of miniaturized domains, it is necessary to resolve diffraction spots from individual microdomains of different orientation variants that compose the macrodomain plates shown in Fig. 1(a). The positions of these diffraction spots would provide the crystal lattice parameters of individual microdomains. Splitting from individual microdomains will only be resolved when the high resolution diffraction condition $H\epsilon_0\lambda_0 \gg 1$, where **H** is the reciprocal lattice vector of the diffraction spot, is met.[19] If this optical condition is not met (i.e., $H\epsilon_0\lambda_0 < 1$), diffraction will be unable to resolve individual microdomains. The crystal lattice parameters obtained using such ''low-resolution'' diffraction represent an averaged lattice, obtained from multiple microdomains that compose the macrodomain plates. In this case, groups (or colonies) of microdomains will be perceived

as a macrodomain of a structurally homogeneous adaptive phase. The lattice parameters of the adaptive phase are then determined by the positions of these low-resolution diffraction spots.

A. Crystal lattice parameters of an adaptive phase consisting of tetragonal microdomains

If the adaptive state is composed of tetragonal microdomains, then the microdomains self-assemble to eliminate the transformation-induced stress. Stress-accommodating microdomains are a particular case of a martensitic structure, which can be described by the Wechsler–Lieberman–Read[1] and Bowles–MacKenzie[2] crystallographic theory of the martensitic transformation. According to this theory, the domain-averaged stress-free transformation strain is an IPS. The theory of adaptive martensite/ferroelectric phases conformally miniaturizes this geometrical theory to the nanoscale. This conformal miniaturization results in the condition that the lattice parameters are predicted by the IPS.

A fully stress-accommodating macrodomain of the adaptive phase consists of two types of tetragonal microdomains with different orientations. These domains are $(110)_c$ twin related to avoid the crystal lattice misfits and to form alternating layers along the $(110)_c$ plane. The tetragonal axes of the layers alternate along the $[100]_c$ and $[010]_c$ directions of the cubic parent phase [as shown in Fig. 1(a)]. The two types of domains formed from the cubic parent phase by stress-free tetragonal deformations are

$$\epsilon(1)=\begin{bmatrix}\epsilon_3 & 0 & 0\\ 0 & \epsilon_1 & 0\\ 0 & 0 & \epsilon_1\end{bmatrix} \quad \text{and} \quad \epsilon(2)=\begin{bmatrix}\epsilon_1 & 0 & 0\\ 0 & \epsilon_3 & 0\\ 0 & 0 & \epsilon_1\end{bmatrix}, \tag{2}$$

where $\epsilon_3=(c_t-a_c)/a_c$ and $\epsilon_1=(a_t-a_c)/a_c$ are the stress-free transformation strains, c_t and a_t are the crystal lattice parameters of the stress-free tetragonal martensite, and a_c is the lattice parameter of the high temperature cubic phase. These matrices are presented in the Cartesian coordinate system where the *x*, *y*, and *z* axes are chosen to be parallel to the cubic directions $[100]_c$, $[010]_c$, and $[001]_c$, respectively. This alternating layered structure of domains (which is illustrated in Fig. 1) can be (and usually is) interpreted as a structure formed by the periodical $(110)_c$ twinning of the tetragonal phase. The thickness of the $\epsilon(1)$ domains is $d_1=\omega\lambda$, where λ is the distance between nearest twins and ω is the volume fraction of the martensite plate occupied by the twin with transformation strain $\epsilon(1)$. The thickness of the lamellar domains of the second orientation variant of the martensite formed by the $\epsilon(2)$ transformation strain is $d_2=(1-\omega)\lambda$.

If the tetragonal strains defined in Eq. (2) are small (i.e., $|\epsilon_1|\ll 1$ and $|\epsilon_3|\ll 1$), then the microdomain-averaged stress-free strain is

$$\begin{aligned}\langle\epsilon(\omega)\rangle &= \omega\epsilon(1)+(1-\omega)\epsilon(2)\\ &= \omega\begin{bmatrix}\epsilon_3 & 0 & 0\\ 0 & \epsilon_1 & 0\\ 0 & 0 & \epsilon_1\end{bmatrix}+(1-\omega)\begin{bmatrix}\epsilon_1 & 0 & 0\\ 0 & \epsilon_3 & 0\\ 0 & 0 & \epsilon_1\end{bmatrix}\\ &= \begin{bmatrix}\epsilon_1+(\epsilon_3-\epsilon_1)\omega & 0 & 0\\ 0 & \epsilon_3-(\epsilon_3-\epsilon_1)\omega & 0\\ 0 & 0 & \epsilon_1\end{bmatrix}.\end{aligned} \tag{3}$$

To eliminate crystal lattice misfits between variants and thus generation of stress, these two variants [$\epsilon(1)$ and $\epsilon(2)$] form alternating twin-related lamellas along the twin plane $(110)_c$. The microdomain-averaged crystal lattice parameters of the adaptive phase, obtained by application of the stress-free strain matrix given in Eq. (3), have pseudo-orthorhombic symmetry. These lattice parameters referenced to the cubic axes [$\mathbf{a}_1=(a_1,0,0)_c$, $\mathbf{a}_2=(0,a_1,0)_c$, $\mathbf{a}_3=(0,0,a_1)_c$] are

$$a_{\mathrm{ad}}=a_t+(c_t-a_t)\omega, \quad b_{\mathrm{ad}}=c_t-(c_t-a_t)\omega, \quad c_{\mathrm{ad}}=a_t, \tag{4}$$

where, by definition, these lattice parameters are directed along the $\langle 100\rangle_c$ axes. Equation (4) is a fingerprint that the system consists of tetragonal microdomains of two orientation variants with the tetragonality axes along the $[100]_c$ and $[010]_c$ axes. It is the crystallographic fulfillment of the conformal miniaturization of the domain variants, which is illustrated in Fig. 1(a).

However, Eq. (4) does not eliminate the stress generated by misfits along the habit plane of the macrodomains. To achieve this condition, the system must choose a special value $\omega=\omega_0$ that provides an IPS. Then, complete strain accommodation is achieved between macrodomain plates of the adaptive phase, and the entire specimen exists in a stress-free condition. This is what we designate the condition of ''strong'' or special invariance, and is the conformal miniaturization of Fig. 1(b). The strain in Eq. (3) is the IPS if one of the diagonal elements of the tensor (3) is zero (in this case, we choose $\langle\epsilon(\omega)\rangle_{11}=0$; if we choose $\langle\epsilon(\omega)\rangle_{22}=0$, we get the crystallographically equivalent variant of the IPS symmetry related to the first one). Then, the domain structure is completely stress accommodating. This condition gives $\omega=\omega_0$, where ω_0 is

$$\omega_0=\frac{\epsilon_1}{\epsilon_1-\epsilon_3}=\frac{a_t-a_c}{a_t-c_t}. \tag{5}$$

Substituting ω_0 into Eq. (4) provides the lattice parameters of the completely stress-accommodating adaptive phase, produced from the parent cubic lattice parameters by the IPS. These parameters are

$$a_{\mathrm{ad}}=a_c, \quad b_{\mathrm{ad}}=c_t+a_t-a_c, \quad c_{\mathrm{ad}}=a_t. \tag{6}$$

The ratio of thicknesses of the twin-related tetragonal microdomains in the stress-accommodating state is then $\omega_0/(1-\omega_0)=(a_t-a_c)/(a_c-c_t)$. In fact, the adaptive phase obtained by averaging over microdomains is monoclinic. However, the monoclinic distortion angle ϕ has been ne-

glected in this pseudo-orthorhombic representation of the crystal lattice parameters of the adaptive phase, as it is proportional to $(\epsilon_3-\epsilon_1)^2$, and thus very small.

It is important to realize that the relations between the crystal lattice parameters of the adaptive, tetragonal, and cubic phases given by Eq. (6) are a particular case of the relations given by Eq. (4): Eqs. (6) are valid only for the particular case of a fully accommodating adaptive phase that has zero applied external fields (i.e., $\omega=\omega_0$). Therefore, Eq. (6) imposes more strong constraint on the crystal lattice parameters of the adaptive phase than Eq. (4). This strong constraint is lifted under applied field, affecting the geometrical parameter ω, which in turn, is determined by the complex energy balance caused by coupling the applied field and domain structure. In this case, $\omega\neq\omega_0$ and the crystal lattice parameters are determined by Eq. (4).

B. Invariants for adaptive phases consisting of tetragonal microdomains

Unlike conventional phases whose crystal lattice constants are intrinsic material constants, the crystal lattice parameters of an adaptive phase are self-adjusting parameters. Self-adjustment provides accommodation of the transformation stress, establishing the invariance condition determined in Eq. (6).

Changes of **E** or σ will result in microdomain rearrangement, characterized by the geometrical parameter ω. This results in a violation of complete stress accommodation (or an increase in the transformation-induced strain energy) at the expense of a decrease in the electrostatic or the total strain energies. Nevertheless, the theory of adaptive phases predicts certain invariant relations for the lattice parameters, which result from requiring the multilayer polytwin structure to be maintained.

Equation (4) describes the situation where the microdomain volume fraction assumes an arbitrary value ω, and consequently does not provide an IPS (i.e., full stress accommodation). In this case, we have the easily verifiable relations

$$a_{\mathrm{ad}}+b_{\mathrm{ad}}=a_t+c_t, \tag{7a}$$

$$c_{\mathrm{ad}}=a_t. \tag{7b}$$

Equations (7a) and (7b) are general: both the crystal lattice parameters of the adaptive phase determined by the partial stress accommodation [see Eq. (4)] and the crystal lattice parameters determined by the full stress accommodation [see Eq. (6)] meet Eqs. (7a) and (7b).

The lattice parameters of the tetragonal phase (a_t and c_t) are intrinsic constants of a conventional phase; they are determined by atomic bonds and are functions of composition and temperature, and are weakly dependent on **E** and σ, whereas, the parameters of the adaptive phase ($a_{\mathrm{ad}}, b_{\mathrm{ad}}, c_{\mathrm{ad}}$) are self-adjusting parameters; they are very sensitive to **E** and σ, and to the distribution of microdomains. However, as follows from Eqs. (7a) and (7b), the sum of the self-adjustable parameters, a_{ad} and b_{ad}, and the value c_{ad}, are also intrinsic physical parameters of the conventional tetragonal phase. Therefore, Eqs. (7a) and (7b) provide invariance conditions. Their left-hand sides are invariants that are independent of the applied field, irrespective of the strong dependences of the adaptive phase parameters a_{ad} and b_{ad} on field. In other words, although separately, a_{ad} and b_{ad} can change pronouncedly with T, **E**, and σ; but, taken additively as given in Eq. (7a), they become invariant. This invariance can be also rewritten as

$$\frac{a_{\mathrm{ad}}+b_{\mathrm{ad}}}{a_t+c_t}=1. \tag{7c}$$

The invariance relations (7a)–(7c) are easily verifiable by experiment for any intermediate pseudo-orthorhombic phase. It is barely possible that their fulfillment is coincidental at fixed temperature, composition, **E** and σ. It is practically impossible that their continued fulfillment over the entire temperature, composition, **E** and σ would be coincidental. Below we will call the conditions of Eqs. (7a)–(7c) the general invariance conditions.

III. PREDICTIONS AND CONFIRMING OBSERVATIONS OF AN ADAPTIVE PHASE FORMED FROM TETRAGONAL MICRODOMAINS

A. Intermediate phases in martensitic transformations

Martensitic phases can be identified as the adaptive type based on the invariant conditions of Eq. (6) and/or (7a)–(7c). Previously, it has been shown that the $7R$ phase in the NiAl alloy and the intermediate phase in the Fe–Pd alloy have a pseudo-orthorhombic phase, whose crystal lattice parameters are adaptive, and satisfy Eq. (6) to a high degree of accuracy.[7,8] This agreement between the measured and calculated parameters shows that the $7R$ phase of NiAl and the intermediate phase of Fe–Pd are adaptive phases. It also validates the assumption that the tetragonal twin-related microdomains have the same crystal lattice parameters as the tetragonal phase.

The measured crystal lattice parameters of the high-temperature cubic phase, low-temperature tetragonal martensitic phase and intermediate orthorhombic (adaptive) martensitic phase for the Fe–Pd alloy[10] are shown in Fig. 2(a). Dots and triangles correspond to the measured points in Ref. 10. A thin line is used to show the predicted adaptive phase lattice parameter $b_{\mathrm{ad}}=c_t+a_t-a_c$, which was calculated by extrapolating the parameters c_t, a_t and a_c. Good agreement can be seen between the predicted adaptive phase lattice parameter and that experimentally observed for the intermediate phase of Fe–Pd. In addition, Fig. 2(a) shows that the a_t lattice parameter of the tetragonal phase transforms smoothly to the c_{ad} parameter of the intermediate pseudo-orthorhombic phase, and that the a_c parameter of the cubic phase transforms smoothly to the corresponding a_{ad} parameter. All of these experimental observations are in a complete agreement with the special invariance conditions of Eq. (6). Figure 2(b) illustrates an excellent fulfillment of the general invariancy condition of Eq. (7a). (This demonstrates that the intermediate orthorhombic phase of Fe–Pd is of the adaptive type, consisting of miniaturized tetragonal microdomains.)

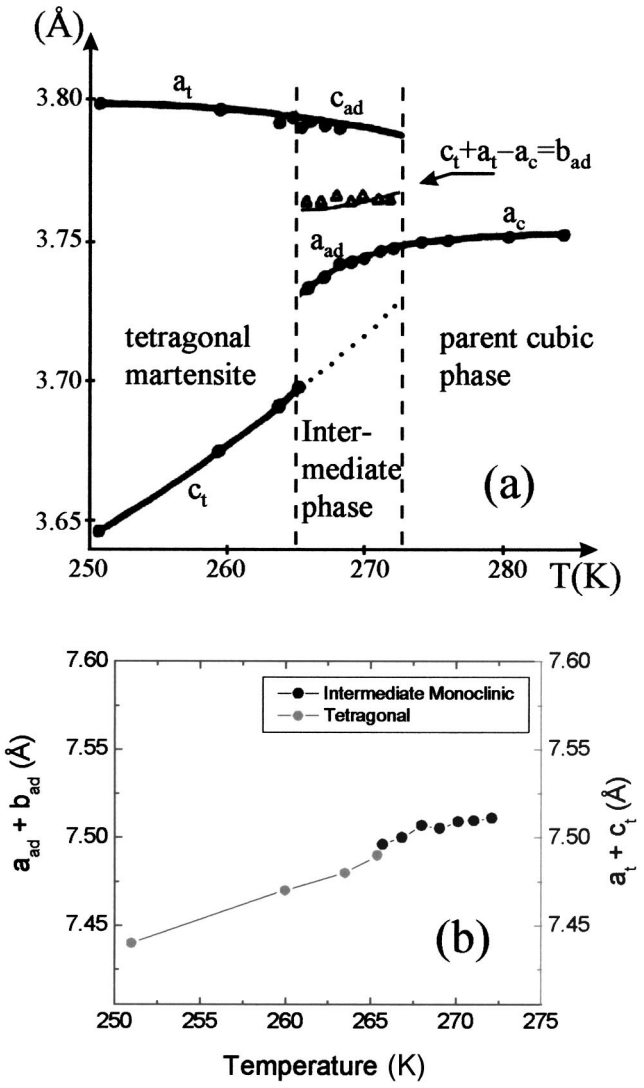

FIG. 2. (a) Temperature dependence of crystal lattice parameters of cubic parent phase, intermediate orthorhombic and tetragonal martensitic phases for Fe–Pd alloy (see Ref. 10). Dots and triangles correspond to the measured points. Thin line in the orthorhombic phase stability region describes $b_{ad}=c_t+a_t-a_c$, dotted line is an extrapolation of a_c to the orthorhombic phase region. (b) Temperature dependence of the adaptive phase invariance [Eq. (7a), $a_{ad}+b_{ad}=a_t+c_t$] illustrating the fulfillment of the invariance requirement. The data for the orthorhombic phase are plotted in black and for the tetragonal phase in gray.

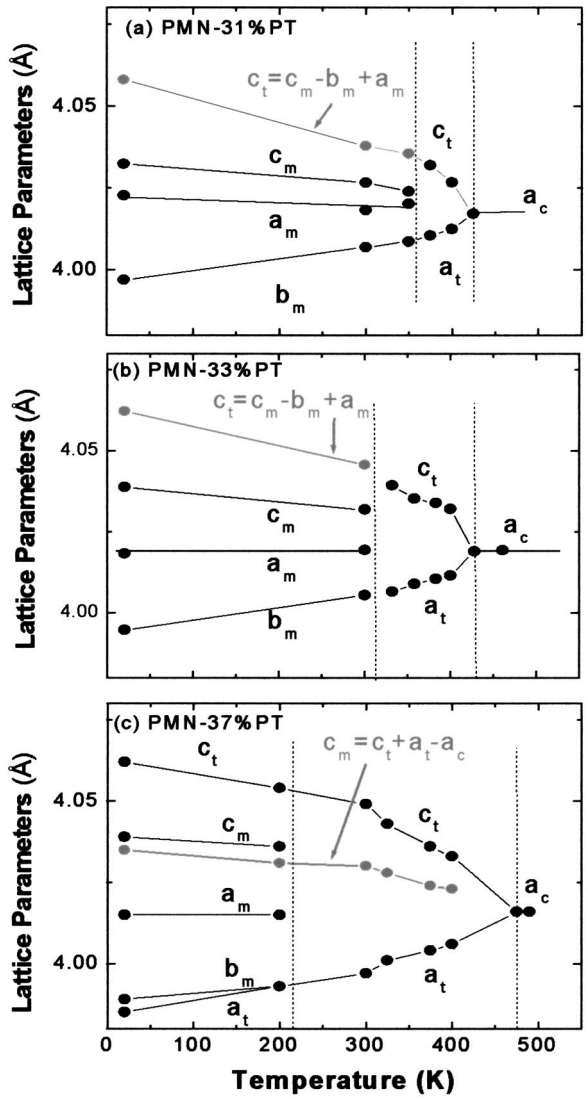

FIG. 3. Temperature-dependent lattice parameters for (a) PMN–31%PT, (b) PMN–33%PT, and (c) PMN–37%PT. These data were taken by neutron diffraction by Noheda *et al.* (see Ref. 11). The points and lines in gray are the lattice parameters calculated by Eq. (8a): (a) and (b) $c_t=c_m-b_m+a_m$ of the tetragonal phase; (c) $c_m=c_t+a_t-a_c$ of the monoclinic phase.

B. FE_m phases in ferroelectrics consisting of tetragonal microdomains

The invariance conditions are also fulfilled for the recently discovered FE_m phases of PMN–x%PT and PZN–x%PT. This composition lies on the MPB between FE_r and FE_t phases, where the domain wall energy is expected to be small. If we use the adaptive phase parameters (a_{ad}, c_{ad}, b_{ad}) of Eq. (6) to designate the FE_m (pseudo-orthorhombic) lattice parameters as ($a_m=a_{ad}$, $b_m=c_{ad}$, $c_m=b_{ad}$), then the special invariance conditions of Eq. (6) can be rewritten as

$$a_m=a_c, \quad b_m=a_t, \quad c_m=c_t+a_t-a_c. \tag{8a}$$

The parameters corresponding to the general invariance conditions of Eqs. (4) and (7a) and (7b) can be rewritten as

$$a_m=a_t+(c_t-a_t)\omega, \quad b_m=a_t, \quad c_m=c_t-(c_t-a_t)\omega, \tag{8b}$$

$$a_m+c_m=a_t+c_t, \quad b_m=a_t. \tag{8c}$$

Both the special and general invariance conditions given in Eqs. (8a) and (8c), respectively, should be preserved with changing temperature, if the FE_m phase remains adaptive. Temperature-dependent neutron diffraction data has previously been obtained for various PMN–xPT powders,[13,14] in the compositional range of $31\%<x<37\%$. These investigations were performed under zero electric field. Thus, any change in the invariance conditions can be attributed solely to the effect of temperature. The data confirm that both the special and general invariance conditions are preserved over a significant temperature range.

Figures 3(a)–3(c) show the temperature dependence of the lattice constants for PMN–31%PT, PMN–33%PT, and

PMN–37%PT, respectively. The tetragonal lattice parameters (a_t,c_t) and cubic lattice parameter (a_c) are shown in the Figs. 3(a)–3(c) in their respective stability ranges. At lower temperatures, the data demonstrate the presence of a FE_m phase with $c_m \neq b_m \neq a_m$. The special ''invariance'' condition of Eq. (8a) was found to be well maintained. To illustrate that this invariance is preserved, the lattice parameter c_t of the metastable tetragonal phase within the stability field of the monoclinic phase was calculated using the relationship $c_t = c_m - b_m + a_m$, which can be obtained by rearranging Eq. (8a) following from the adaptivity theory. The calculated values of c_t are plotted in gray, alongside the measured ones of the FE_m phase. It can be seen in Figs. 3(a) and 3(b) that the calculated parameter $c_t = c_m - b_m + a_m$ provides a continuous extension of the lattice parameter c_t measured in the stability field of the FE_t phase, extrapolated into the stability field of the FE_m phase. Also, in accordance with the special invariance conditions, the measured lattice parameter b_m of the FE_m phase is a continuous extension of the lattice parameter a_t measured in the stability range of the FE_t phase. Furthermore, the measured lattice parameter a_m is equal to a_c; however, this parameter does not continuously extend between the cubic and FE_m phases. Rather, it undergoes hibernation in the FE_t phase, spontaneously reappearing in the FE_m phase as the parameter a_m, in accordance with the invariance condition $a_m = a_c$. In addition, it is important to note for PMN–37%PT that the FE_m and FE_t phases coexisted over the temperature range of $0 < T < 200$ K. The values of the lattice parameters of the FE_t and FE_m phases were found to be inter-related. One set of parameters could be determined from the other as illustrated by the calculated lattice parameter $c_m = c_t + a_t - a_c$ [see Eq. (8a)] shown by the gray line in Fig. 3(c). Coexistence may reflect the proximity of the composition to the MPB and the small fluctuations in PT content within the crystal.

It should be noted that, according to our model, the formation of the adaptive (monoclinic) phase is not a phase transition in the usual thermodynamic sense: the formation of a usual phase is determined by the balance of the free energies of the parent and product phases, the formation of an adaptive phase is not. The monoclinic adaptive phase is not a conventional crystallographically homogeneous phase either. It is a homogenized mixed state of twin-related tetragonal microdomains. A reason why we call this state a ''phase'' is that at a certain degree of miniaturization of the tetragonal phase domains, the low-resolution x-ray diffraction perceives the tetragonal domain mixture as a homogeneous monoclinic crystal lattice.

The general invariance conditions of Eq. (8c) were found to be well preserved for PMN–xPT, over both wide compositional ($31\% < x < 37\%$) and temperature ($20 < T < 500$ K) ranges. Figure 4 shows fulfillment of the general invariance condition $a_m + c_m = a_t + c_t$ as a function of temperature for the various PMN–xPT compositions. The data clearly demonstrate that the general invariance condition is obeyed over the entire temperature and compositional range of the FE_m and FE_t phase.

Application of **E** induces a violation of the special invariance condition of Eq. (8a), preventing complete stress

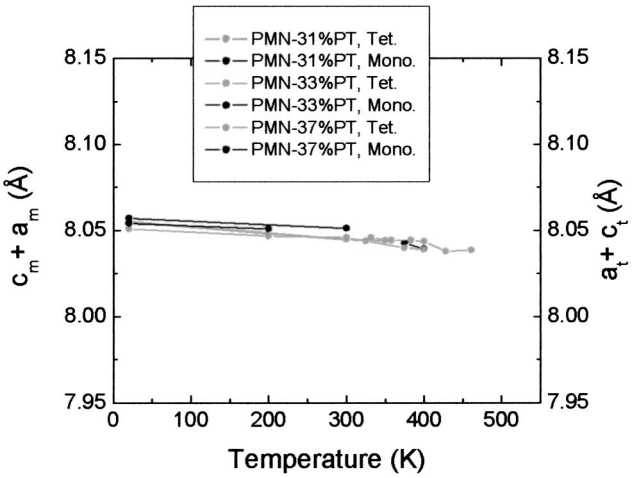

FIG. 4. Temperature dependence of the general invariance condition of Eq. (8c), $a_m + c_m = a_t + c_t$. Data are shown for PMN–31%PT, PMN–33%PT, and PMN–37%PT. The values of $(a_m + c_m)$ and $(a_t + c_t)$ were calculated from corresponding data in Figs. 3(a)–3(c). Please note that data for the monoclinic and tetragonal phase regions are shown in black and gray, respectively.

accommodation. However, the general invariance condition of Eqs. (8b) and (8c) will still be fulfilled, that is if the FE_m phase remains adaptive. The field dependence of the crystal lattice parameters of PZN–8%PT has been determined by single-crystal neutron diffraction.[12,13] Figure 5(a) shows data that prescribe the dependence of the crystal lattice parameters of the FE_m (pseudo-orthorhombic) phase on applied **E**, over the entire FE_m stability range up to the point that the FE_t phase is induced. Figure 5(b) shows the corresponding plot of the general invariance condition of Eq. (8c). The results clearly demonstrate that the general invariance condition is rigidly obeyed over the entire FE_m stability range and into the FE_t phase field. The fulfillment of the predicted general invariance demonstrates that the changes in the lattice parameters with **E** are due to a redistribution of tetragonal microdomains, which are arranged in $(101)_c$ twin-related multilayer patterns. The FE_t phase is reached when the crystal is fully detwinned by the field, which occurs when the geometric ratio in Eq. (8b) is zero, i.e., $\omega = 0$.

Under zero field, for PZN–8%PT, the monoclinic (pseudo-orthorhombic) lattice parameters have the special relationship $a_m = c_m$. When a_m becomes equal to c_m, the symmetry of the lattice increases from monoclinic to orthorhombic. The latter can be seen by using a doubled orthorhombic unit cell in a manner similar to that for orthorhombic $BaTiO_3$ (Refs. 20 and 21) rather than a monoclinically distorted primitive cell of the host cubic lattice. We designate this orthorhombic phase as FE_O. In this case, Eq. (8b) still describes this orthorhombic phase as a particular case where the relative volume fractions of the microdomain variants is $\omega = 1/2$ and the $(101)_c$ twin-related tetragonal microdomains are $(101)_c$ atomic layers with equal thickness $a_c/\sqrt{2}$. In fact, investigations of poled $(110)_c$-oriented crystals have demonstrated that full remanence can be sustained along the $[110]_c$, in agreement with this possibility.[18,22]

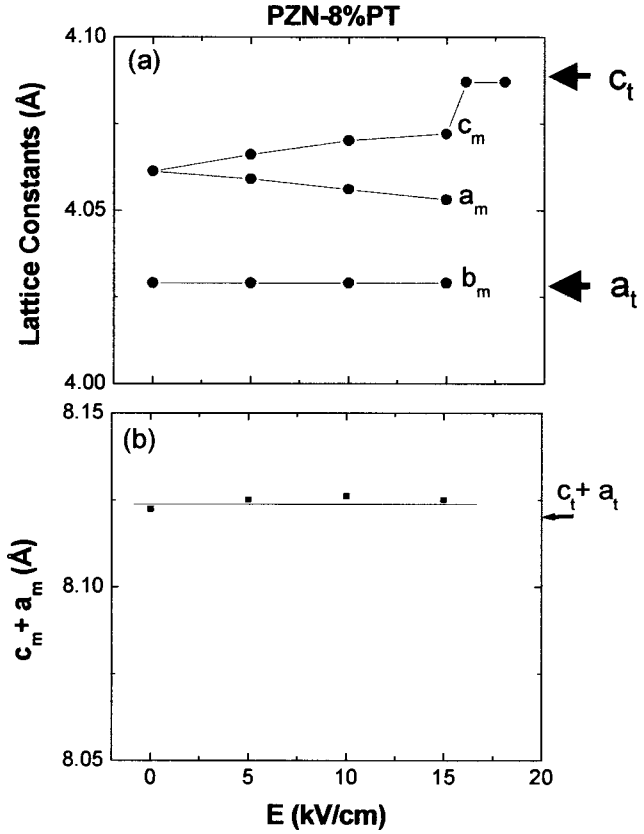

FIG. 5. (a) Dependence of the crystal lattice parameters, c_m, a_m, and b_m, of the pseudo-orthorhombic (monoclinic) phase in PZN–8%PT on the applied electric field (see Refs. 12 and 13). (b) Dependence of the sum, $a_m + c_m$, on **E**. The independence of this sum on **E** is the fulfillment of the invariance condition of Eq. (8c). The results demonstrate that $a_m + c_m = a_t + c_t$, as required by the general invariance condition.

The locking of ω into the particular value $\omega = 1/2$ corresponding to the formation of the orthorhombic phase can be attributed to interactions between domain walls, which cannot be neglected in the relevant case because the separation distance between the walls is of atomic scale. By and only at this special geometrical value $\omega = 1/2$, the symmetry of the system is increased from monoclinic (pseudo-orthorhombic) to orthorhombic. This abrupt increase in symmetry necessitates a singularity in the chemical free energy at $\omega = 1/2$. This singular point can be either the free energy minimum (local or global) or the maximum with respect to ω. The minimum should be an infinitesimally narrow ''pothole'' on the free energy versus ω curve. The observation of this orthorhombic phase, in fact, confirms that the free energy singularity is a free energy minimum, and that the orthorhombic phase is either stable or metastable.

Since $\omega = 1/2$ is not equal to the value ω_0, complete stress accommodation and the special invariance condition are not achieved [Eq. (8a)]. However, the general invariance condition is well maintained under applied field [see Eq. (8c)]. Figure 5 indicates that an applied field unlocks ω from this special value, making $\omega(\mathbf{E}) \neq 1/2$ in Eq. (8b). The fact that the parameters of the unlocked phase fulfill the general invariance of Eq. (8c) demonstrates that both the locked orthorhombic phase FE_O and unlocked monoclinic phase are both described by the adaptive phase theory.

The results clearly show that the general invariance conditions are obeyed over a broad range of electric fields [Fig. 5(b)], temperatures, and compositions (Fig. 4). This continued fulfillment of the invariance conditions over such a broad stability range unambiguously demonstrates that the FE_m phase is not a homogeneous (unique) phase requiring independent lattice parameters. Rather, it is an adaptive phase which can be described over its entire stability range by adjustable parameters, given by the invariance conditions.

C. Extreme piezoelectricity in adaptive ferroelectrics with tetragonal microdomains

Equation (4) describes the situation where ω can deviate from ω_0; in which case, the volume fractions of microdomains do not provide complete stress accommodation. Deviation will occur under applied external fields, which can change the populations of tetragonal microdomains with different orientations, increasing the relative volume fractions of those that are favorably orientated with respect to the applied field. This effect is responsible for the adaptivity of the phase in its response to the applied field. In the case of a ferroelectric adaptive phase, the applied field can be either **E** or σ. In particular, application of **E** will result in a piezoelectric strain, caused by microdomain rearrangement. The piezoelectric tensor $d_{ij,k}$ can be obtained by differentiating the strain tensor (Eq. (3)) with respect to **E**, given as

$$d_{ij,k} = \frac{\partial \langle \epsilon(\omega) \rangle_{ij}}{\partial E_k} = (\epsilon_3 - \epsilon_1) \begin{pmatrix} 1 & 0 & 0 \\ 0 & 0 & 0 \\ 0 & 0 & 1 \end{pmatrix} \frac{\partial \omega}{\partial E_k}. \qquad (9)$$

The piezoelectric effect of an adaptive ferroelectric is determined by the dependence of its crystal lattice parameters on **E**. Since, these crystal lattice parameters form invariant dependency neither on **E** nor on σ, Eq. (9) predicts that there are analogous invariance conditions between the various piezoelectric tensor coefficients. Indeed, Eq. (9) predicts that $d_{11,i} = -d_{33,i}$. The piezoelectric properties of PZN–8%PT were calculated from the field dependence of the lattice parameter data shown in Fig. 5(a). The piezoelectric coefficients $d_{11,i}$, $d_{22,i}$, and $d_{33,i}$ are shown in Fig. 6 as a function of the field. The results confirm that $d_{33,i} = -d_{11,i} = 4500$ pC/N, and that $d_{22,i} = 0$.

These results demonstrate that the unique piezoelectric properties of the FE_m phase of PZN–8%PT can be described by the adjustable parameters of an adaptive ferroelectric state consisting of tetragonal microdomains. This is a natural consequence of the faithful adherence to the general invariance conditions of Eq. (8c). Accordingly, energy can readily be transduced from electrical to mechanical form by the redistribution of microdomain variant populations upon application of **E**, and vice versa upon application of σ.

D. Polarization of an adaptive ferroelectric phase, and its rotation under *E*

If the adaptive phase is ferroelectric, then each tetragonal microdomain must have a polarization. Let us assume that the polarization of a tetragonal microdomain is directed

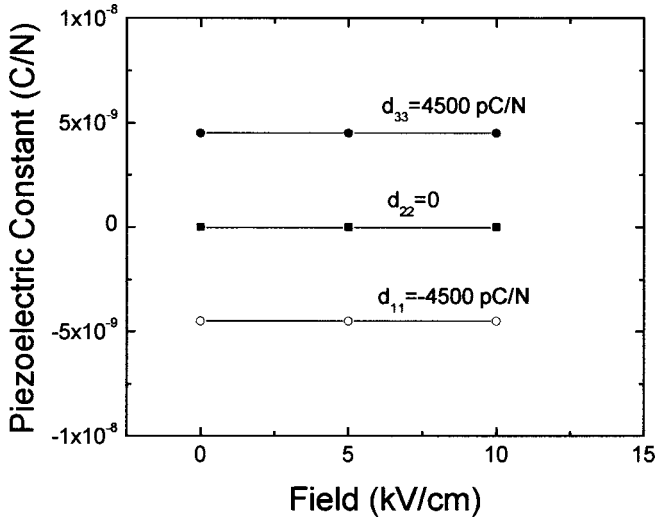

FIG. 6. Piezoelectric coefficients $d_{11,i}$, $d_{22,i}$, and $d_{33,i}$ for PZN–8%PT as a function of electric field illustrating the relations predicted by Eq. (9).

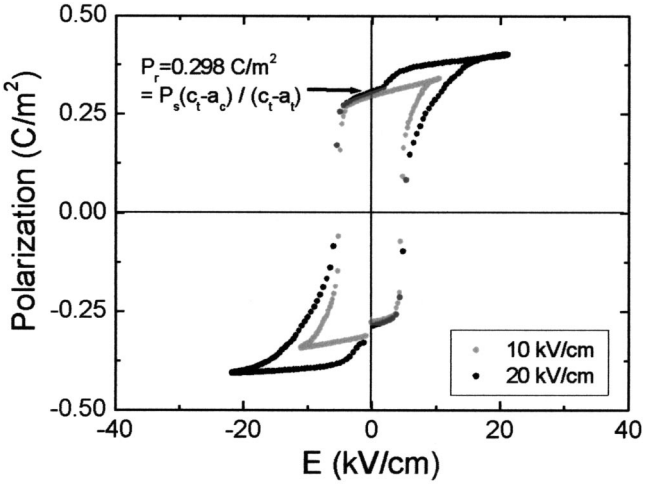

FIG. 7. $P-E$ hysteresis loop for a $(001)_c$-oriented PZN–8%PT. A remanent polarization of 0.298 C/m^2 is obtained upon removal of the field. The saturation polarization was 0.41 C/m^2. These data were taken from Ref. 18.

along the c axis. With certainty, we can assume: (i) that the microdomains have the same geometrical arrangement as shown in the previous section, i.e., $(101)_c$ twin-related tetragonal microdomains of two orientational variants that form an IPS plate; and (ii) that the tetragonal microdomains have their c axes oriented along $[100]_c$ and $[001]_c$, where the other crystallographically equivalent variants can be obtained by application of cubic symmetry rotations and reflections. Based upon these two assumptions, the components of the polarization vectors in the microdomains of the first and second orientation variants are $\mathbf{P}(1)=(P_s,0,0)_c$ and $\mathbf{P}(2)=(0,0,P_s)_c$, respectively, where P_s is the saturation polarization of the FE_t phase. These vectors are presented in a Cartesian coordinate system, and are referenced to the $\langle 100\rangle_c$ direction of the high temperature cubic phase.

The total polarization of the adaptive (pseudo-orthorhombic) ferroelectric phase can be obtained by averaging that of the tetragonal microdomains over the volume of the macrodomain plate of the adaptive phase. If the volume fraction of the domains of the first orientation is ω and the fraction of the domains of the second type is $(1-\omega)$, then the microdomain polarization averaged over the macrodomain of the adaptive phase is

$$\mathbf{P}=\omega\mathbf{P}(1)+(1-\omega)\mathbf{P}(2)=\omega(P_s,0,0)_c+(1-\omega)(0,0,P_s)_c$$
$$=P_s(\omega,0,1-\omega)_c. \tag{10a}$$

The total polarization is the absolute value of the vector of Eq. (10a), and is equal to

$$P_T=P_s\sqrt{\omega^2+(1-\omega)^2}. \tag{10b}$$

It is important to notice that in the case of a fully detwinned tetragonal ferroelectric phase ($\omega=0$ or $\omega=1$), P_T is equal to the saturation polarization of the tetragonal phase P_s. It follows from Eq. (10a) that the total polarization vector, $\mathbf{P}$, rotates in the $(010)_c$ plane if ω changes. Equation (10b) demonstrates that the norm of the total polarization, P_T, is also a function of ω. Since the electric field induces microdomain rearrangement that changes ω, an application of the electric field $\mathbf{E}$ should rotate the polarization vector in the $(010)_c$ plane changing its norm. The application of external stress or clamping should have the similar effect on the polarization.

In the completely stress-accommodating state and in the absence of an applied electric field and external stress, the geometric volume fraction is $\omega=\omega_0$, as given Eq. (5). Substituting Eq. (5) into Eq. (10a) gives the remanent polarization of the adaptive (pseudo-orthorhombic) phase as

$$\mathbf{P}_{\mathbf{E}=0}=\frac{P_s}{\epsilon_1-\epsilon_3}(\epsilon_1,0,-\epsilon_3)$$
$$=\frac{P_s}{a_t-c_t}[(a_t-a_c),0,-(c_t-a_c)]. \tag{11}$$

Equation (11) predicts that the remanent polarization ($\mathbf{P}_{\mathbf{E}=0}$) of a macrodomain state of the stress-accommodating adaptive phase is determined by the crystal lattice parameters of the paraelectric phase and ferroelectric tetragonal phase of microdomains. For PZN–8%PT, we can predict the value of the remanent polarization using the crystal lattice parameters, $(a_t,c_t)=(4.032,4.089)$ Å, the cubic lattice parameter for this composition $a_c=4.047$ Å,[12,13] and the saturation polarization of the tetragonal phase $P_s=0.41$ C/m^2 taken from Ref. 18 as

$$\mathbf{P}_{\mathbf{E}=0}=\frac{0.41}{-0.057}(-0.015,0,-0.042)$$
$$=(0.108,0,0.302)\ \text{C/m}^2. \tag{12}$$

Figure 7 shows the polarization hysteresis ($P-E$) loop for a $(001)_c$-oriented PZN–8%PT crystal. These $P-E$ data were obtained from different PZN–8%PT specimens[18] than that of the neutron data of Fig. 5.[12,13] From this hysteresis loop, the remanent polarization projected onto the $(001)_c$ direction can be determined to be 0.298 C/m^2. This is very close to the value 0.302 C/m^2 predicted by Eq. (12). In this case, complete stress accommodation is restored after removal of electric field.

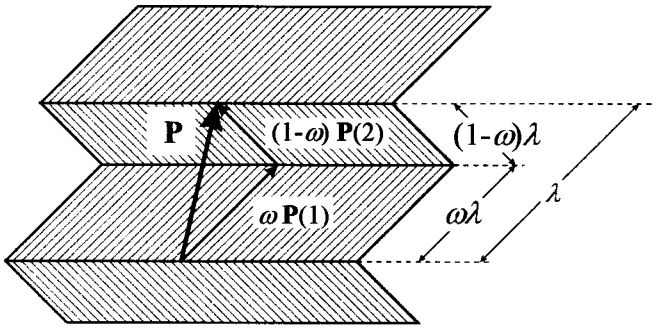

FIG. 8. Microdomain-averaged polarization of the adaptive ferroelectric consisting of twin-related microdomains of the tetragonal ferroelectric phase with the polarizations **P**(1) and **P**(2). The microstructure is in the $(010)_c$ plane section. This adaptive phase is a miniaturized 90° ferroelectric domain structure. The directions of hatching indicate the directions of the tetragonality axes. The thin arrows indicate the polarization within microdomains weighted by the volume fractions of these microdomains. The thick arrow indicates the resultant polarization of the adaptive phase.

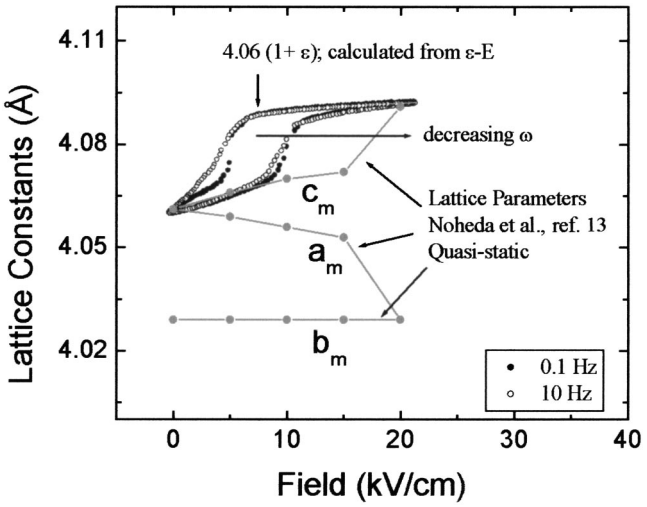

FIG. 9. Lattice parameters for PZN–8%PT as a function of electric field. The data in gray were taken by neutron diffraction (see Refs. 12 and 13). The data in black show the lattice parameter c_m calculated from the electrically induced strain (ϵ–**E**) response at different frequencies from the relationship $c_m = 4.06(1+\epsilon)$.

In the absence of applied field, the volume fraction ω of microdomains composing a macrodomain of the adaptive phase is equal to ω_0, which is given by Eq. (5). When $\omega = \omega_0$, the strain energy is minimized by achievement of stress accommodation. Only under these conditions is the polarization given by Eq. (11). In the more general case of an arbitrary ω, the net polarization **P** is given by Eq. (10a). For this general case, an important conclusion can be reached: *the polarization vector of the adaptive phase consisting of* $(101)_c$ *twin-related microdomains is restricted to lie in the* $(010)_c$ *plane of the parent cubic lattice of the paraelectric phase, irrespective of the relative volume fractions of microdomains*.

For conventional uniaxial ferroelectrics, the saturation polarization and its direction are fixed at a given temperature, with the polarization vector bound to an easy direction. However, for an adaptive ferroelectric phase, this is not the case. It follows from Eqs. (10a) and (10b), that in the adaptive phase, *the magnitude and direction of the polarization vector* **P** *is determined by the ratio of the thicknesses of microtwins. This is illustrated in Fig. 8. As shown in this illustration, the polarization vector gradually rotates with a gradual change of the microdomain volume fraction* ω. Application of **E** changes the value of ω, due to an increase in the volume fraction of the favorably oriented microdomains, at the expense of unfavorably oriented ones. Therefore, $\omega = \omega(\mathbf{E})$ is a variable dependent on the magnitude and direction of **E**. According to Eqs. (10a) and (10b), a change in ω changes the absolute value and direction of the net polarization **P**. The polarization vector will gradually rotate in the $(010)_c$ plane with a gradual change in **E**. This rotation will continue until the unfavorably oriented microdomains entirely disappear at $\omega = 0$. Then, **P** lies along the $[001]_c$. This condition corresponds to the complete detwinning of the microtwinned plates, and the transformation of the adaptive monoclinic (pseudo-orthorhombic) phase into the conventional FE_t.

E. Shape memory effects and slim-loop hysteresis in adaptive ferroelectrics

Similar to shape memory alloys, the strain obtained by application of σ to an adaptive phase will be close to the stress-free transformation strain, which is orders of magnitude higher than that of the Hookean strain of most conventional solids. If the adaptive phase is ferroelectric, then shape memory will also be observed by application of **E**. An important distinction of the adaptive phase is that domain walls are much more mobile than in conventional martensite, which is due to the small γ. Microdomain populations will be changed by σ and **E**, resulting in shape changes, which will be recovered upon removal of the field. Thus, the adaptive phase will have significantly narrower strain–stress (ϵ–σ) and strain–field (ϵ–**E**) hysteresis loops.

The electrically induced strain for a $(001)_c$-oriented PZN–8%PT crystal was measured using a conventional ϵ–**E** hysteresis method. Measurement frequencies of 0.1 and 10 Hz were used. The value of the c_m lattice parameter for $(001)_c$-oriented PZN–8%PT under zero field is 4.06 Å [see Fig. 5(a)]. The c_m lattice parameter was then approximated from the ϵ–**E** curve by the relationship $c_m = 4.06(l+\epsilon)$ Å. This approach to calculate the lattice constants is not valid for conventional ferroelectrics, as the induced strain characteristics are related to electrically induced shape changes from domain contributions, rather than inherent changes in lattice constants. However, in an adaptive ferroelectric phase, the shape changes from domain contributions are directly related to those of the adaptive (pseudo-orthorhombic) lattice, as the microdomain-averaged lattice parameters follow the twinning rules.

The calculated values of $c_m = 4.06(1+\epsilon)$ are shown in Fig. 9 as a function of E. We designate these data as c_m–E hysteresis curves, to remind the reader of how they were derived. Shape memory is clearly evident upon removal of the electric field, as the pseudo-orthorhombic fully stress-

accommodating state is remembered after removal of field. Lattice parameters determined by neutron diffraction are shown alongside the c_m-E hysteresis curves. Similarities are obvious between the dynamic c_m-E hysteresis curve and the quasistatic field-dependent values of c_m determined by neutron diffraction in Fig. 9. Also, with decreasing frequency, the hysteresis in the c_m-E curve was noticeably decreased, becoming increasingly slim looped and more similar to those determined by neutron diffraction.

IV. DISCUSSION AND SUMMARY

In this article, the theory of a single-phase ferroelectric domain structure has been extended to the particular case where the domain wall energy γ is abnormally low. In this case, the sizes of domains proportional to $\sqrt{\gamma}$ [Eq. (1)] is drastically reduced and ferroelectric domains are conformally miniaturized. This is the main assumption of our theory. We believe that this assumption is realistic near a MPB between two ferroelectric perovskite-based phases with different orientations of the polarization vector. This assumption has several significant ramifications.

First, there will be a conformal miniaturization of the domain structure, without a significant change in the topology of the spatial pattern or distribution of variant populations. The domain topology is not affected because miniaturization is driven by the vanishing of the volume-dependent elastic strain and depolarization energies: it is not dependent on the surface energy contributions from domain boundaries. There are two important intrinsic length parameters, which control the size of the domain structure. These are $\gamma/\mu\epsilon_0^2$ and γ/P_s^2, which are both proportional to γ and are reduced to the nano- and subnanoscale under the condition of drastically small γ.

Second, conformal miniaturization of domains results in a structurally inhomogeneous phase on a scale less than 10 nm. Whereas, on length scales >10 nm, the structure appears homogeneous unless the high resolution diffraction is used. Indeed, locally (within microdomains), the structure is tetragonal; however, the microdomain-averaged lattice is pseudo-orthorhombic. In order to resolve the crystal lattice parameters of individual microdomains, the optical condition $H\epsilon_0\lambda_0 \gg 1$ must be met where $\mathbf{H}=(H,K,L)$ is the reciprocal lattice vector of the operational diffraction spot, and (H,K,L) are the indexes. This estimate can be rewritten as

$$\lambda_0 \gg \frac{a_0}{\epsilon_0\sqrt{H^2+K^2+L^2}}. \tag{13}$$

Using the experimental values of $\epsilon_0=\epsilon_3-\epsilon_1\sim 10^{-2}$ and assuming a high reflection index of $\sqrt{H^2+K^2+L^2}\sim 10$, we can estimate using Eq. (13) that microdomains will be resolvable if $\lambda_0 \gg 10a_0$. Diffraction patterns taken under low resolution will perceive the lattice parameters as those of the pseudo-orthorhmbic periodical homogeneous lattice, the values of these parameters being microdomain averaged. To perceive that of individual microdomains, the sum must be $H^2+K^2+L^2 \gg 10^2$. This estimate indicates that microdomains can reach ten(s) of nanometers and still not be resolved. We designate this structurally mixed state as the adaptive ferroelectric phase. The unique properties of the adaptive ferroelectric phase are due to the fact that it is a macroscopically homogeneous phase, which on the nanometer scale has both an inhomogeneous structure and polarization.

Third, the lattice parameters of the adaptive phase are a mixture of those of the parent cubic and low temperature product ones. They are not intrinsic physical constants, rather they are parameters that are adjusted to achieve stress and depolarization electric field accommodation. Adjustments occur by changes in microdomain variant populations. Under the condition of complete stress accommodation, the crystal lattice rearrangement transforming the paraelectric phase to the adaptive ferroelectric one is the IPS. The special and general invariance conditions of the crystal lattice parameters of the adaptive phase are the fingerprints of the adaptivity. The general invariance condition [see Eqs. (7a)–(7c)] achieves stress accommodation by eliminating misfits between variants. The special invariance condition [see Eq. (6)] does this also, but in addition, it eliminates misfits along the habit plane of the macrodomain. These invariance conditions imposed on the crystal lattice parameters are so restrictive and special that it is certainly impossible that their continued fulfillment over an entire temperature, concentration, electric field, and stress stability ranges of an intermediate phase is coincidental.

In the case of an adaptive ferroelectric phase consisting of tetragonal microdomains, the microdomain-averaged symmetry is monoclinic (pseudo-orthorhombic). Under the condition of full stress accommodation, crystal lattice parameters of the pseudo-orthorhombic adaptive phase have the following special crystallographic relationship with the cubic and tetragonal ones: $a_{\mathrm{ad}}=a_c$, $b_{\mathrm{ad}}=c_t+a_t-a_c$, and $c_{\mathrm{ad}}=a_t$. These special relations are easily verified, and have been done for martensitic transformations in Ni–Al (Ref. 9) and Fe–Pd (Ref. 10) alloys, and for PMN–PT ferroelectric crystals.

Fourth, normally one considers the polarization as the order parameter of a ferroelectric phase, where the electrostriction is a cross-coupled product that is only an improper ferroelastic response. However, in an adaptive ferroelectric state, the coelastic nature of the solid is much more significant. This is because of the important role of stress-accommodating microdomains, which results in a microdomain-averaged polarization. The polarization of individual microdomains is either tetragonal or rhombohedral. However, unlike conventional ferroelectrics, the microdomain-averaged polarization is not bound to an easy direction; rather, it depends upon the microdomain distribution. Accordingly, the polarization vector can gradually rotate if the relative volume fractions of microdomains with different orientations are changed by an application of σ and $\mathbf{E}$. In the case of tetragonal microdomains, it has been demonstrated that the polarization gradually rotates in the $\{100\}_c$ planes with gradual change in σ and $\mathbf{E}$. The theory of adaptive ferroelectric states predicts the direction and magnitude of the polarization as given in Eqs. (10a) and (10b), and shown in Fig. 8.

Fifth, the reduction of the value of γ lowers the energy

cost of the structure and polarization transformation within a domain wall, and thus reduces the domain wall energy. Therefore, for $\gamma \to 0$, the energy of the crystal lattice reconstruction and polarization change occurring during domain wall movement vanishes or is drastically reduced. This will increase the domain wall mobility remarkably, as there will be little or no barrier for domain transformation or domain wall movement under the applied field. Accordingly, slim $P-E$ and $\epsilon-E$ responses will be observed.

We have also recently found that an adaptive ferroelectric phase can be formed from rhombohedral microdomains. (We will publish these results separately, once the calculations are fully completed.) At this time, it is important to mention that the stress-accommodating rhombohedral microdomains also result in an adaptive monoclinic phase. However, this monoclinic phase is different from that formed by tetragonal microdomains. The orientation relation between the rhombohedral microdomain-averaged monoclinic adaptive state and the cubic parent phase is $(010)_m \| (1\bar{1}0)_c$. The monoclinic parameters a_m, b_m, and c_m are close to the $[110]_c$, $[1\bar{1}0]_c$, and $[001]_c$ directions of the parent cubic lattice, respectively. Their values are $a_m \sim \sqrt{2}a_c$ along $[110]_c$, $b_m \sim \sqrt{2}a_c$ along $[1\bar{1}0]_c$, and $c_m \sim a_c$ along $[001]_c$. In the particular case where the paraelectric→rhombohedral ferroelectric transition does not result in volume change (i.e, a special invariance is observed), the monoclinic phase becomes orthorhombic. Similar to the case of an adaptive phase formed from tetragonal microdomains, the polarization vector in an adaptive phase formed from rhombohedral microdomains also gradually rotates with gradual change in **E**. However, the rotation in the latter case occurs in the $\{110\}_c$ planes.

Finally, it should be mentioned that the adaptive phase theory of ferroelectrics formulated here neglects the intrinsic piezoelectric strain of tetragonal microdomains. This assumption is supported by the fact that the intrinsic piezoelectic strain is much smaller than that caused by the field-induced microdomain structure rearrangement. Rearrangement of microdomains results in a strain on the order of 10^{-2}, and makes monoclinic adaptive ferroelectric phases promising acoustic and energy transduction materials. Taking the intrinsic piezoelectric distortion into account is very simple, although it would result in certain algebraic complications: we would have to modify Eq. (2) by adding to the transformation strain the field-dependent piezoelectric strain of the tetragonal phase.

ACKNOWLEDGMENTS

Three of the authors (Y.M.J., Y.U.W., and A.G.K.) gratefully acknowledge the support of the NSF under Grant No. DMR-0242619. Two of the authors (J.F.L. and D.V.) gratefully acknowledge the support of ONR under Grant Nos. N000140210340, N000140210126, and MURI N000140110761.

[1] M. S. Wechsler, D. S. Lieberman, and T. A. Read, Trans. J. Metals **197**, 1503 (1953).
[2] J. C. Bowles and J. K. Mackenzie, Acta Metall. **2**, 129 (1954).
[3] A. G. Khachaturyan and G. A. Shatalov, Zh. Eksp. Teor. Fiz. **56**, 1037 (1969) [Sov. Phys. JETP **29**, 557 (1969)].
[4] A. G. Khachaturyan, *The Theory of Structural Transformations in Solids* (Wiley, New York, 1983).
[5] A. L. Roytburd, Fiz. Tverd. Tela (Leningrad) **10**, 3619 (1968) [Sov. Phys. Solid State **10**, 2870 (1969)].
[6] V. I. Syutkina and E. S. Jakovleva, Phys. Status Solidi **21**, 465 (1967).
[7] A. G. Khachaturyan, S. M. Shapiro, and S. Semenovskaya, Phys. Rev. B **43**, 10 832 (1991).
[8] A. G. Khachaturyan, S. M. Shapiro, and S. Semenovskaya, Mater. Trans., JIM **33**, 278 (1992).
[9] S. M. Shapiro, B. X. Yang, G. Shirane, Y. Noda, and L. E. Tanner, Phys. Rev. Lett. **62**, 161 (1989).
[10] H. Seto, K. Noda, and Y. Yamada, J. Phys. Soc. Jpn. **59**, 965 (1990).
[11] B. Noheda, D. Cox, G. Shirane, J. Gao, and Z. Ye, Phys. Rev. B **63**, 54104 (2002).
[12] K. Ohwada, K. Hirota, P. W. Rehrig, P. M. Gehring, B. Noheda, Y. Fujii, S. E. Park, and G. Shirane, J. Phys. Soc. Jpn. **70**, 2778 (2001).
[13] B. Noheda, J. A. Gonzalo, L. E. Cross, R. Guo, S. E. Park, D. E. Cox, and G. Shirane, Phys. Rev. B **61**, 8687 (2000).
[14] B. Noheda, D. Cox, G. Shirane, J. Gonzalo, and L. E. Cross, Appl. Phys. Lett. **74**, 2059 (1999).
[15] S. Park and T. R. Shrout, J. Appl. Phys. **82**, 1804 (1997).
[16] J. Kuwata, K. Uchino, and S. Nomura, Jpn. J. Appl. Phys., Part 1 **21**, 1298 (1982).
[17] D. Viehland and J. Powers, Appl. Phys. Lett. **78**, 3112 (2001).
[18] D. Viehland, J. Appl. Phys. **88**, 4794 (2000).
[19] A. G. Khachaturyan, Kristallografiya **4**, 646 (1959).
[20] J. Merz, Phys. Rev. **76**, 1221 (1949).
[21] H. Kay and P. Vousden, Philos. Mag. **40**, 1019 (1949).
[22] Y. Lu, Q. M. Zhang, and D. Viehland, Appl. Phys. Lett. **78**, 3109 (2001).